WITHDRAWN: Glioblastoma cell-derived extracellular vesicle miR-27a-3p facilitates M2 macrophage polarization

Guifang Zhao
the Sixth Affiliated Hospital of Guangzhou Medical University, Qingyuan People's Hospital; Jilin Medical University
Hongquan Yu
the First Hospital of Jilin University
Lijuan Ding
the First Hospital of Jilin University
Weiyao Wang
Jilin Medical University
Huang Wang
the Sixth Affiliated Hospital of Guangzhou Medical University, Qingyuan People's Hospital
Yao Hu
the Sixth Affiliated Hospital of Guangzhou Medical University, Qingyuan People's Hospital
Lingsha Qin
the Sixth Affiliated Hospital of Guangzhou Medical University, Qingyuan People's Hospital
Guangce Deng
the Sixth Affiliated Hospital of Guangzhou Medical University, Qingyuan People's Hospital
Buqing Xie
the Sixth Affiliated Hospital of Guangzhou Medical University, Qingyuan People's Hospital
Guofeng Li
the Sixth Affiliated Hospital of Guangzhou Medical University, Qingyuan People's Hospital
Lin Qi
qilingip@126.com

the Sixth Affiliated Hospital of Guangzhou Medical University; Jilin Medical University

Research

Keywords: Glioblastoma, Extracellular vesicles, microRNA-27a-3p, Enhancer of zeste homologue 1, M2 macrophage polarization

Posted Date: May 1st, 2020

DOI: https://doi.org/10.21203/rs.3.rs-24999/v1

EDITORIAL NOTE:

The full text of this preprint has been withdrawn by the authors while they make corrections to the work. Therefore, the authors do not wish this work to be cited as a reference. Questions should be directed to the corresponding author.

Abstract

Background: M2 macrophage polarization has been found to be correlated with malignancy of glioblastoma. In this study, we investigated the potential role of microRNA (miRNA) derived from extracellular vesicles of glioblastoma (glioblastoma-EVs) in M2 macrophage polarization.

Methods: After isolation of human glioblastoma-EVs, transmission electron microscopy (TEM) and Nano-particle tracking analysis (NTA) were performed to identify the EVs. Besides, the proliferation, migration and invasion of glioma cells were analyzed by CCK8 and Transwell assays, respectively. The target genes of miR-27a-3p were predicted through bioinformatics analysis and verified by dual-luciferase reporter gene assay. ChIP assay was applied to detect the binding of enhancer of zeste homologue 1 (EZH1) to lysine-specific demethylase 3A (KDM3A) promoter region and the interaction between KDM3A and connective tissue growth factor (CTGF). Glioblastoma mouse models were established followed by the implement of hematoxylin-eosin (HE) and ELISA staining on pathological changes of mouse brain tissues.

Results: Human glioblastoma-EVs were successfully isolated. The high expression of miR-27a-3p was found in glioblastoma tissues as well as glioblastoma-EVs, which could induce M2 polarization, thus promoting glioblastoma cell proliferation, migration and invasion. It was also shown that miR-27a-3p targeted EZH1 and promoted KDM3A expression to elevate the expression of CTGF. Glioblastoma-EVs delivered miR-27a-3p to promote the KDM3A-upregulated CTGF by downregulating EZH1, thereby promoting M2 macrophage polarization and development of glioblastoma *in vivo.*

Conclusion: These findings highlight that EV miR-27a-3p may promote M2 macrophage polarization, which is associated with the progression of tumors.

Background

Glioblastoma is the most lethal type of glioma with aggressive brain tumors and often occurred in individuals older than 65 years [1, 2]. Moreover, the median survival of glioblastoma is less than two years [3], which is in urgent need of novel treatment modalities. Tumor-associated M2 macrophages is reported to play a central role in tumor development [4]. Hypoxia and M2-like macrophages are correlated with poor prognosis of glioblastoma [5]. Therefore, to investigate the M2 macrophage-modulated tumor microenvironment of glioblastoma may represent a prognostic biomarker for glioblastoma. It is reported that the extracellular vesicles of glioblastoma (glioblastoma-EVs) carry functional genomic and proteomic cargo and affect surrounding and distant recipient cells, which enables EVs to emerge as crucial mediators of tumor microenvironment in glioblastoma [6]. Previous work also highlights the promoting role of microRNAs (miRNAs) delivered by glioblastoma-EVs in M2 macrophage polarization [7]. However, the miRNAs derived from glioblastoma-EVs are not fully understood, and it is necessary to further explore the detailed function of glioblastoma-EVs carried miRNA in M2 macrophage polarization.

miRNAs are small non-coding RNAs which are implicated in different physiological processes, and dysregulation of miRNAs can lead to various cancers [8]. miRNAs can be EVs' components playing signaling role in the progression of cancers [9]. miR-27a-3p has been revealed to be involved in the development of glioma [10]. Furthermore, hsa-miR-27a-3p has been found to be enriched in circulating EVs [11]. However, few studies analyzed the effects of miR-27a-3p derived from glioblastoma-EVs on glioblastoma and the relevant tumor microenvironment. Additionally, enhancer of zeste homologue 1 (EZH1) is strikingly downregulated in glioblastoma, which may play a role in the development of glioblastoma [12]. What's more, EZH1 is able to suppress the polarization of M2 macrophage [13]. This study aims to analyze the relationship between miR-27aa-3p carried in glioblastoma-EVs and the underlying regulatory mechanism to provide better understanding of glioblastoma and gain functional insights into the glioblastoma-EVs mediated miRNAs. To grasp EVs-modulated tumor microenvironment may unveil novel diagnostic and therapeutic targets for glioblastoma.

Methods And Materials

Ethical statement and study object

The usage of cerebrospinal fluid and tumor tissues was approved by the Institutional review board (IRB) of the Jilin University. The study protocol was authorized by the IRB of the Jilin University. with patient's written informed consent obtained. This study was performed in compliance with the *Declaration of Helsinki*. The animal experiments were approved by the Animal Ethics Committee of the Jilin University.

Glioblastoma tissue samples used in this study were collected from glioblastoma patients (n = 50) who underwent surgical treatment in the oncological neurosurgery department of the First Hospital of Jilin University from June 2016 to June 2019. Sample controls were obtained from non-glioblastoma patients (n = 20) with encephalopathy.

Cell culture and transfection

Human glioblastoma cell line U87MG, human monocyte cell line U937 and murine glioblastoma cell line GL261 were provided by the Institute of Biochemistry and Cell Biology, Chinese Academy of Sciences. U87MG cells were cultured in Dulbecco's modified eagle medium (DMEM; Thermo Fisher Scientific, Waltham, MA, USA) containing 10% fetal bovine serum (FBS). Meanwhile, U937 cells were cultured in Roswell Park Memorial Institute (RPMI)-1640 medium (Thermo Fisher Scientific) with 10% FBS, which were further incubated with 100 ng/mL phorbol-myristate-acetate (PMA) (Sigma-Aldrich, St. Louis, MO, USA) for 24 h *in vitro* to induce the differentiation into macrophages. Additionally, 1 μg/mL EV was added to the medium of recipient cells for co-culture with EVs. All cell lines were identified by short tandem repeat (STR) and confirmed to be mycoplasma negative before the experiments. Small interfering RNA (siRNA), miRNA inhibitor/mimic and virus vectors were purchased from GenePharma (Shanghai, China).

Isolation of EVs

Cells were cultured in 10% EV-FBS-free DMEM (A2720801, GIBCO BRL, Green Island, NY, USA) under normoxia (21% O_2) or hypoxia (1% O_2). After 48–72 h of incubation, the culture medium was collected and the EVs were separated by ultracentrifugation. The EVs were isolated following the detailed procedures as previously described [7]. Human glioblastoma-EVs or murine glioblastoma-EVs were isolated using the Exoquick ULTRA EV Isolation Kit (EQULTRA-20A-1, System Biosciences, Irvine, CA, USA).

Transmission electron microscope (TEM)

The EV obtained by high-speed centrifugation of 400 mL medium was fixed in 2% glutaraldehyde overnight at 4℃, washed with PBS, fixed with 1% OsO_4 for 1 h, dehydrated in ethanol and embedded with epoxy resin. Embedded-sections were added with saturated sodium periodate and 0.1 N hydrochloric acid, the size and morphological characteristics of which were observed using TEM (JEM-1010; JEOL, Tokyo, Japan) after 10 min.

Mixed with 4% paraformaldehyde, EVs were placed on the Formvar carbon coated Electron Microscopy (EM) grid, followed by the acquisition of Images using TEM (Hitachi, Tokyo, Japan). The EV surface marker proteins rabbit anti-CD63 (ab134045, 1:1000, Abcam, Cambeidge, UK), rabbit anti-Tsg101 (ab125011, 1:1000, Abcam, UK) and rabbit anti-Calnexin (ab92573, 1:20000, Abcam, UK) were determined using Western blotting while the particle size and concentration of EVs were analyzed using QNano (Izon Sciences Ltd, NZ).

Nano-particle tracking analysis

The size distribution and concentration of EVs were determined following the instructions of NTA (Zetasizer Nano ZS90 instrument, Malvern, UK), which associated with light scattering and Brownian motion. PBS-diluted EVs were injected into Zetasizer Nano ZS90 instrument, followed by the measurement of particle size according to Brownian motion and diffusion coefficient. The filtered PBS was used as a control. All samples were measured using NP100 film with 44.5 mm and 0.64 V voltage parameters. Samples were calibrated by the dilution of CPC100 standard particles at 1,000 times under the same condition. With 5 videos (60-s-duration) taken, data were analyzed using Zetasizer software (Malvern) to identify and track each particle.

EV labeling and immunofluorescence

EVs with the concentration of 0.1–0.2 μg were resuspended in 400 μL PBS and stained with CellMask Deep Red (Thermo Fisher Scientific) at excitation/emission wavelengths of 649/666 nm. During the labeling, EVs were incubated with deep red staining solution (1:1000) for 20 min at 37℃. Then EVs were centrifuged at 100,000 g for 1 h and diluted in PBS, followed by the determination of protein concentration using bicinchoninic acid (BCA) protein detection kit.

Cells were stained with CellTrace™ Carboxyfluorescein succinimidyl ester (CFSE, Life Technologies, Carlsbad, CA, USA) with a maximum excitation/emission wavelength of 492/517 nm. The

immunofluorescence staining was performed after the covalent binding of cells diffused by lactone-digested CFSE with intracellular amines. Glioblastoma cells ($3–5 \times 10^5$) in serum-free medium were stained with CFSE (working concentration of 5 μM) at a dilution of 1:1000 and incubated at 37℃ for 20 min in the dark. After cells were seeded into 8-well slides (Millipore, Billerica, MA, USA), EVs were incubated with CFSE-stained cells at different time points. Cells were fixed with 3.7% (w/v) formaldehyde for 5 min at room temperature, imaged and observed under a fluorescence microscope.

Chromatin immunoprecipitation (ChIP)

Cells were treated using the EpiQuik Tissue ChIP Kit (48 reactions) (P-2003-2, Epigentek, USA). Confluent cells at 70–80% confluency were fixed with 1% formaldehyde at room temperature for 10 min to generate the intracellular DNA-protein crosslink, which was then randomly broken by ultra-sonication into fragments. Cell fragments were centrifuged at 13,000 g at 4℃, followed by the division of supernatant into three tubes, respectively, which was separately added with antibody RNA polymerase II (positive control), mouse antibody immunoglobulin G (IgG) (1 mg/mL) or rabbit IgG (3900, Cell Signaling Technology, USA) (negative control) or antibodies against KDM3A (ab91252, Abcam, Cambridge, UK), H3K27me3 (ab1220, Abcam, UK), CTGF (SimpleChIP Human CTGF Promoter Primers #14927, USA), H3K27ac (ab4729, Abcam) and H3K4me1 (ab8895, Abcam). After immunoprecipitation, de-crosslink was performed and proteins were treated by proteinase K. DNA was eluted and purified using Active Motif's ChIP DNA purification kit (58002, Millipore). Each experiment was repeated 3 times.

Western blotting

Proteins were extracted from tissues or cells while cells were detached in RIPA lysis buffer (Beyotime Biotechnology, Shanghai, China). Total protein concentration was quantified using BCA method, followed by the separation of proteins using 10% sodium dodecyl sulfate-polyacrylamide gel electrophoresis (SDS-PAGE). Separated proteins were transferred onto a polyvinylidene fluoride membrane (Millipore), which was blocked by 5% milk powder containing 0.1% Tween-20. Membrane was incubated with primary antibodies including rabbit anti-EZH1 (ab64850, 1:1000, Abcam), mouse anti-KDM3A (ab91252, 1:1000, Abcam), rabbit anti-CTGF (ab6992, 1:1000, Abcam), rabbit anti-iNOS (ab3523, 1:500, Abcam), rabbit anti-Arg-1 (93668, 1:1000, Cell signaling technology) and rabbit anti-β-actin (ab179467, 1:5000, Abcam) overnight at 4℃. Subsequently, membrane was further incubated with horseradish peroxide (HRP) labeled secondary antibody goat anti-rabbit IgG (ab205718, 1:5000, Abcam) or goat anti-mouse IgG (ab205719, 1:5000, Abcam) at room temperature for 2 h. Protein bands were developed with enhanced chemiluminescence reagent (BB-3501, Amesham, UK), and image analysis was performed in an imaging system (Bio-Rad, Hercules, CA, USA) with β-actin functioned as an internal reference. Each experiment was repeated 3 times.

RNA isolation and quantification

According to the instructions of the Trizol reagent (Invitrogen, Carlsbad, CA, USA), RNA was extracted, which was reversely transcribed into complementary DNA (cDNA) using the first strand cDNA synthesis kit (Tiangen Biotech, Beijing, China) or Primer script™ one-step RT-PCR Kit (Takara, Shiga, Japan). Real-

time polymerase chain reaction was conducted in ABI 7500 real-time PCR system (Applied Biosystems, Carlsbad, CA, USA) using SYBR Green IReal-time PCR kit (Cowin Bioscience, Beijng, China) with GAPDH or U6 used as an internal reference. Cel-miR-39 (No. miRB00000010-3-1 and MQPS0000071-1-100, Riobio, Guangzhou, China) was used as an external reference for the detection of EV miR-27a-3p. The relative expression of genes was analyzed by $2^{-\Delta\Delta CT}$ method, and primers involved in this experiment were shown in Table 1.

Table 1
Primer sequences for RT-qPCR

	Human	Mouse
miR-27a-3p	F 5-'GCGCGTTCACAGTGGCTAAG – 3'	
	R 5-'AGTGCAGGGTCCGAGGTATT – 3'	
U6	F 5-'AGAGAAGATTAGCATGGCCCCTG – 3'	
	R 5-'AGTGCAGGGTCCGAGGTATT – 3'	
EZH1	F 5-'CGAGTCTTCCACGGCACCTA – 3'	F 5-'CTCAGTGGCAACATGCCTAA – 3'
	R 5-'GCAAACTGAAAGACCTGCTTGC – 3'	R 5-'CCCACAAACACAACCAACAG – 3'
KDM3A	F 5-'TTCTTTTCCTCCAAGATTCCC – 3'	F 5-'CCAGGAGAAGACTTCAGAGACATG – 3'
	R 5-'GGGACCATTCGAGCTGTTT – 3'	R 5-'GGTGTACTCAGGCAGTGGAATG – 3'
CTGF	F 5-'TCAACCTCAGACACTGGTTTCG – 3'	F 5-'AGCCAACTGCCTGGTCCAGA – 3'
	R 5-'TAGAGCAGGTCTGTCTGCAAGC – 3'	R 5-'CGCAGAACTTAGCCCTGTATGT – 3'
IL-10	F 5-'GCTCCTAGAGCTGCGGACT – 3'	F 5-'TGGACAACATACTGCTAACCGAC – 3'
	R 5-'TGTTGTCCAGCTGGTCCTTT – 3'	R 5-'CCTGGGGCATCACTTCTACC – 3'
TNFα	F 5-'GCCTGCTGCACTTTGGAGTG – 3'	F 5-'AAGCCTGTAGCCCACGTCGTA – 3'
	R 5-'TCGGGGTTCGAGAAGATGAT – 3'	R 5-'GGCACCACTAGTTGGTTGTCTTTG – 3'
β-actin	F5-'ATCGTGCGTGACATTAAGGAGAAG – 3'	F 5-'AGATCAAGATCATTGCTCCTCCT – 3'
	R 5-'AGGAAGGAAGGCTGGAAGAGTG – 3'	R 5-'AGATCAAGATCATTGCTCCTCCT – 3'

Notes: F, Forward; R, Reverse; EZH1, enhancer of zeste 1; KDM3A, lysine demethylase 3A; CTGF, connective tissue growth factor; RT-qPCR, reverse transcription quantitative polymerase chain reaction

Cell counting kit-8 (CCK-8) assay

The proliferative capacity of glioblastoma cells was detected using CCK-8 kit (Dojindo, Kumamoto, Japan) according to the instructions. Glioblastoma cells were seeded in 96-well plates for co-culture with

different EVs at 0, 24, 48 and 72 h. CCK-8 solution was added to each well, which was incubated for 2 h. Then, the viable cells were measured at the optimal density (OD) of 450 nm using a microplate (Multiskan Sky Microplate Spectrophoto-meter, Cat. No. 51119570, Thermo Fisher Scientific). Each experiment was repeated 3 times.

Transwell assay

The migration and invasion ability of glioblastoma cells was evaluated using Transwell assay by following the manufacturer's protocol. Matrigel (BD Bioscience, Franklin Lakes, NJ, USA) coated apical Transwell chambers were placed at 37℃ for 30 min to polymerize Matrigel. Cells were cultured in serum-free medium for 12 h, harvested and resuspended in serum-free medium (1×10^5/mL). While 100 μL cell suspension was incubated in the basolateral chamber containing 10% FBS at 37℃ for 24 h. Cells that did not invade the surface of Matrigel membrane were gently removed with cotton swabs. Cells were fixed with 100% methanol and stained with 1% toluidine blue (Sigma-Aldrich). Stained cells were counted in five randomly selected areas under inverted light microscope (Carl Zeiss, German). Each experiment was repeated 3 times.

Dual-luciferase reporter gene assay

EZH1 3'-untranslated region (UTR) sequences containing binding sites with mutant type(MUT) or wild type (WT) miR-27a-3p were constructed by Genscript (Nanjing, China). Both EZH1 3'-UTR MUT and WT were cloned into pGL-3 luciferase reporter plasmids. HEK293T cells were cultured in 24-well plates for 24 h, which were then co-transfected with pGL-3-WT-EZH1 or pGL-3-MUT-EZH1 3'-UTR reporter plasmids, internal reference plasmids and miR-27a-3p mimic or mimic NC using Lipofectamine 3000 (Invitrogen, USA). Renilla luciferase activity and Firefly luciferase activity were measured by dual luciferase assay system (Promega, Madison, WI, USA) with Renilla luciferase as internal reference. The experiment was repeated 3 times.

Animal experiment

BALB/c female nude mice (n = 60) were purchased from SLAC Laboratory Animal (Shanghai, China). After 1-week adaptive feeding, mice were anesthetized with pentobarbital sodium and treated differently with 12 mice in each treatment. Sham-operated mice were taken as the sham group, while others were injected through the brain with murine glioblastoma cell line GL261 (with 10^6 cells each mouse) or macrophage (with 2×10^5 cells each mouse) with adenovirus-mediated CTGF knockdown. Subsequently, mice in each group were intravenously injected with PBS or the equivalent volume of EV (8 mg/kg) extracted from miR-27a-3p mimic-treated GL261 cells *via* the caudal vein every 3 days. Six mice were randomly selected from each group to record the survival time. The tumors of other mice were dissected 40 days after xenograft, frozen in liquid nitrogen or fixed in formalin, with serum samples collected.

Enzyme-linked immunosorbent assay (ELISA)

ELISA kits involving hsa-interlukin (IL)-10 (ab46034, Abcam), mmu-IL-10 (ab46103, Abcam), hsa-TNF-α (ab100654, Abcam) and mmu-TNF-α (ab208348, Abcam) were commercially obtained to detect the levels

of IL-10 and TNF-α in the supernatant of U87-MG cells and peripheral blood of mice. Each well of the 96-well microtitration plates was added with 100 μL IL-10 or TNF-α (0.4 μg/mL) buffer solution and 50 mM sodium carbonate to adjust the pH value to 9.6. After overnight incubation at 4℃, the plate was blocked by PBS containing 1% BSA for 1 h at room temperature. IL-10 or TNF-a antibodies or samples to be tested were added to the wells, which were then incubated at room temperature for 2 h. Plates were incubated with 0.2 μg/mL biotinylated IL-10 or TNF-α antibodies for 2 h at room temperature. Diluted peroxidase-labeled antibiotic protein (1:1000; Sigma-Aldrich) was incubated with the plate for 1 h at room temperature. The chromogenic reaction was induced by the addition of 3,3',5,5'-tetramethylbenzidine (TMB)/H_2O_2 substrate solution, which was terminated by 1 M phosphoric acid after 30 min. The OD was measured at 450 nm wavelength using an automatic microplate reader. The OD value was measured with normalization to diluted antibodies in the medium, ranging from 10 to 2,000 pg/mL with standard curves plotted.

Hematoxylin-Eosin (HE) staining

Mouse brain tissues were fixed in 10% formalin for 24 h, routinely dehydrated and paraffin-embedded. Brain tissue samples were cut into 3 μm-thick sections and HE staining was performed following previously described methods [14] to determine the lesion areas in mouse brain tissues. The images were photographed under a microscope at 100-fold magnification.

Statistical analysis

All data were analyzed using SPSS 21.0 software (SPSS, Inc, Armonk, NY, USA). Measurement data were expressed by mean ± standard deviation. Unpaired *t*-test was used for comparison between two groups, while one-way analysis of variance (ANOVA) was used for comparison among multiple groups and Tukey's post hoc test. Comparison among groups at different time points was conducted using two-way ANOVA and Bonferroni's post hoc test. A $p < 0.05$ was considered statistically significant.

Results

Glioblastoma-EVs induce M2 macrophage polarization under hypoxia condition

To explore whether glioblastoma-EVs promote M2 macrophage polarization under hypoxia condition, glioblastoma-EVs were extracted from the supernatant of cultured human glioblastoma cell line U87MG, which were analyzed by TEM, NTA and Western blotting. The results showed that glioblastoma-EVs were typical round particles expressing CD63 and TSG101 proteins instead of calnexin proteins, which were with an average diameter of 105 ± 5.8 nm (Fig. 1A-1C). Meanwhile, human monocyte cell line U937 was treated with PMA to induce the differentiation into macrophages. Following that, macrophages were stained with CFSE while glioblastoma-EVs were stained with deep red staining solution. Subsequently, the stained glioblastoma-EVs were co-cultured with CFSE-stained macrophages under normoxia or hypoxia conditions, respectively. After 24-h co-culture, it was found through the fluorescence microscope that

macrophages would adhere to and took in glioblastoma-EVs, and under hypoxia condition macrophages could take in more glioblastoma-EVs (Fig. 1D).

To further determine that glioblastoma-EVs can induce M2 macrophage polarization under hypoxia, RT-qPCR was performed on the expression of M1 macrophage marker IL-10 and M2 macrophage marker TNF-α. Also, the secretion levels were analyzed by ELISA. The results showed that compared with the control group, the expression of IL-10 under hypoxia was increased while the TNF-α expression was suppressed. Moreover, glioblastoma-EVs under hypoxic significantly increased the secretion of IL-10 in macrophages, but prominently reduced the secretion of TNF-α, confirming that it is more likely that glioblastoma-EVs induce M2 macrophage polarization under hypoxic condition than normoxic condition (Fig. 1E-1F).

Glioblastoma-EVs transfer miR-27a-3p to promote M2 macrophage polarization

Furthermore, we found that the expression of miR-27a-3p in glioblastoma was significantly increased in glioblastoma-related microarray GSE65626 which was obtained from GEO database (https://www.ncbi.nlm.nih.gov/geo/) (Fig. 2A), and the expression of miR-27a-3p was also found to be increased in clinical specimens (Fig. 2B). Therefore, we explored the role of miR-27a-3p in glioblastoma-EVs-induced M2 macrophage polarization under hypoxia. The expression of miR-27a-3p was determined in macrophages incubated with glioblastoma-EVs under hypoxia or normoxia. Compared with macrophages under normoxia, miR-27a-3p showed higher expression in macrophages under hypoxia (Fig. 2C). Together with the results shown in Fig. 1D, these results suggested that miR-27a-3p could be delivered to macrophages by glioblastoma-EVs. Subsequently, macrophages were transfected with miR-27a-3p mimic or miR-27a-3p inhibitor and then cultured under normoxia or hypoxia. The expression of miR-27a-3p, IL-10 and TNF-α in each group was detected by RT-qPCR, the results of which showed that IL-10 expression was increased and TNF-α expression was decreased after treatment of miR-27a-3p mimic under hypoxia/normoxia, while the plasmid miR-27a-3p inhibitor induced the opposite effect. (Fig. 2D-2F). In addition, the expression of macrophage polarization markers iNOS and Arg-1 was evaluated, and the results revealed that iNOS was downregulated and Arg-1 was upregulated in macrophages transfected with miR-27a-3p mimic under hypoxia/normoxia, while the opposite effects were observed in macrophages transfected with miR-27a-3p inhibitor (Fig. 2G-H). These results indicate that upregulation of miR-27a-3p can induce M2 macrophage polarization under hypoxia/normoxia.

Next, the migration, invasion and proliferation of glioblastoma cells were evaluated after co-culture of macrophages with glioblastoma cells. The results of CCK-8 assay showed that the proliferation ability of glioblastoma cells co-cultured with macrophages was strengthened after miR-27a-3p mimic treatment relative to mimic NC, but weakened in glioblastoma cells co-cultured with miR-27a-3p inhibitor-treated macrophages in contrast to inhibitor NC (Fig. 2I). In addition, the results of Transwell assay showed higher motility of glioblastoma cells co-cultured with miR-27a-3p mimic-treated macrophages, while cell motility was curtailed in glioblastoma cells co-cultured with miR-27a-3p inhibitor-treated macrophages

(Fig. 2J-2K). These results indicate that miR-27a-3p can promote the polarization of M2 macrophages, thereby facilitating the proliferation, migration and invasion of glioblastoma cells *in vitro*.

EZH1, the target of miR-27a-3p, inhibits M2 macrophage polarization

We further predicted the downstream target genes of miR-27a-3p through starBase database (http://starbase.sysu.edu.cn/) and mirDIP database (http://ophid.utoronto.ca/mirDIP/index.jsp#r). Meanwhile, differential analysis was performed on the microarrays GSE12657, GSE104291 and GSE50161 using limma package of R language with |logFoldChange| > 1 and *p*-value < 0.05 as threshold. The prediction results of differentially expressed genes and target genes in the differential analysis results were intersected (Fig. 3A). Subsequently, GO functional analysis of intersected genes revealed that those genes were mainly enriched in the pathways of "modulation of chemical synaptic transmission", "neuron to neuron synapase" and "protein serine/threonine kinase activity" (Fig. 3B). The expression of EZH1 was analyzed in the three glioblastoma-related microarrays, showing that EZH1 was reduced. The expression of EZH1 in microarray GSE50161 was shown in Fig. 3C. We further detected the mRNA expression of EZH1 in clinical specimens and found that EZH1 expression was also decreased in glioblastoma patients (Fig. 3D).

According to the prediction of starBase, there existed binding sites between hsa-miR-27a-3p/mmu-miR-27a-3p and EZH1 (Fig. 3E). The targeting relationship between EZH1 and miR-27a-3p was verified using dual-luciferase reporter gene assay, and the results showed that the fluorescence intensity of the cells co-transfected with miR-27a-3p mimic and EZH1 3'UTR-WT decreased significantly (Fig. 3F). To further validate the regulation of EZH1 by miR-27a-3p at the cellular level, U87MG cells were transfected with miR-27a-3p mimic, followed by the extraction of EVs. Then, EVs were co-cultured with macrophages overexpressing EZH1 under hypoxia. Results of RT-qPCR showed that the expression of miR-27a-3p elevated while EZH1 expression was reduced in the miR-27a-3p mimic-treated cells, along with increased IL-10 and decreased TNF-α expression. However, the expression of miR-27a-3p did not significant change in the cells co-transfected with miR-27a-3p mimic and EZH1 overexpression vector (oe-EZH1) and cells co-transfected with miR-27a-3p and oe-NC, while among miR-27a-3p mimic- and oe-EZH1-treated cells the expression of EZH1 and TNF-α increased and IL-10 expression was decreased, indicating that the overexpression of EZH1 reversed the effects of miR-27a-3p on M2 macrophage polarization (Fig. 3G-3I). In addition, the expression of iNOS and Arg-1, the polarization markers of macrophages, was further determined in each group. Results showed that the iNOS expression was decreased and Arg-1 expression was increased after the treatment of miR-27a-3p mimic of miR-27a-3p, while the overexpression of EZH 1 could reverse the effects of the miR-27a-3p mimic (Fig. 3J). The findings suggest that the overexpression of EZH 1 could reverse the expression of miR-27a-3p effects on M2 macrophage polarization.

CCK-8 and Transwell assays were conducted to detect the effects of miR-27a-3p mimic and/or oe-EZH1 on glioblastoma cell proliferation, migration and invasion. The proliferation, migration and invasion of glioblastoma cells were increased after treatment of miR-27a-3p mimic, but were distinctly suppressed

after the addition of oe-EZH1, indicating that the overexpression of EZH1 offset the effects of overexpressed miR-27a-3p on the proliferation (Fig. 3K), migration and invasion (Fig. 3L-3M) of glioblastoma cells. These results indicate that miR-27a-3p induces M2 macrophage polarization by targeting EZH1.

EZH1 inhibits M2 macrophage polarization by suppressing KDM3A expression

As ChIP-Seq data analysis results unraveled, EZH1 was found to bind to the promoter of KDM3A (Fig. 4A), suggesting that EZH1 inhibited KDM3A at a transcriptional level. Next, we performed ChIP analysis using anti-H3K27me3 antibody after si-EZH1 treatment to detect changes of histone modifications. It was found that EZH1 protein was highly enriched in the promoter region of KDM3A after macrophages were treated with 3xFLAG-EZH1 vector (Fig. 4B). Moreover, si-EZH1 significantly enhanced H3K27me3 methylation in the promoter region of KDM3A gene (Fig. 4C). Therefore, endogenous EZH1 protein can bind to the promoter region of KDM3A and inhibit the expression of KDM3A gene by removing histone H3K27me3. It can be inferred that H3K27me3 plays an important role in the activation of the promoter region of KDM3A gene.

To further explore the regulatory relationship between EZH1 and KDM3A, EZH1 or/and KDM3A was knocked down in macrophages. Results of RT-qPCR displayed that silencing EZH1 could upregulate KDM3A, increase IL-10 and decrease TNF-α expression to induce M2 macrophage polarization. While knockdown of KDM3A reversed the effects of silenced EZH1 on M2 macrophage polarization when co-transfected with si-EZH1 (Fig. 4D-4F). Additionally, the results of Western blotting exhibited that silencing EZH1 could downregulate the expression of iNOS and upregulate the expression of Arg-1, while KDM3A knockdown could reverse the effects of silenced EZH1 on M2 polarization (Fig. 4G). These results suggest that EZH1 regulates M2 macrophage polarization by inhibiting KDM3A expression through H3K27me3 methylation.

KDM3A facilitates macrophage polarization by upregulating CTGF

To examine the regulatory function of endogenous KDM3A protein in macrophages, we performed ChIP analysis on cells using antibodies to CTGF, H3K27ac and H3K4me1 after treatment of macrophages with siRNA targeting KDM3A (si-KDM3A). It was found that KDM3A protein was highly enriched in the enhancer region of CTGF gene. Meanwhile, the changes of histone modification in the enhancer region of the gene were also detected. The results displayed that H3K4me1 and H3K27ac were simultaneously enriched in the enhancer region, and activation of enhancers promotes CTGF gene expression. The data also revealed that the degree of H3K4me1 and H3K27ac modification was remarkably elevated after siRNA treatment (Fig. 5A-5B). Therefore, endogenous KDM3A protein can bind to the enhancer region of CTGF and activate enhancers to promote CTGF gene expression by removing histone H3K4me1 and H3K27ac modifications.

To further explore the regulatory relationship between KDM3A and CTGF, KDM3A was overexpressed or/and CTGF was knocked down in macrophages. Results of RT-qPCR exhibited that overexpression of KDM3A upregulated CTGF and IL-10 expression but decreased TNF-α expression to induce M2 macrophage polarization. However, after overexpressing KDM3A or knocking CTGF down in cells, it was found that depleted CTGF could inhibit M2 macrophage polarization which was induced by overexpressed KDM3A (Fig. 5C-5E). The protein expression of macrophage polarization markers iNOS and Arg-1 was further examined in each group. The results showed that overexpression of KDM3A could downregulate iNOS protein expression and upregulate Arg-1 protein expression, while knockdown of CTGF could reverse the M2 macrophage polarization induced by overexpression of KDM3A (Fig. 5F), which was consistent with the above results. These results suggest that KDM3A promotes M2 macrophage polarization by binding to CTGF enhancer regions and promoting CTGF gene expression.

M2 macrophage polarization can be accelerated by glioma-EVs-released miR-27a-3p/EZH1/KDM3A/CTGF in vitro

To determine whether EZH1 can regulate CTGF expression through KDM3A, EZH1 or CTGF was knocked down in macrophages, followed by the detection of EZH1, KDM3A and CTGF expression. It was found that the expression of EZH1 and TNF-α decreased while the expression of KDM3A, CTGF and IL-10 increased after EZH1 was silenced, accompanied with accelerated M2 macrophage polarization. However, the expression of EZH1 and KDM3A did not change significantly in the si-EZH1 and sh-CTGF group compared with the si-EZH1 and sh-NC group, while the expression of CTGF and IL-10 decreased after EZH1 and CTGF were both silenced, along with increased TNF-α expression, indicating that knockdown of CTGF could reverse the M2 macrophage polarization induced by overexpressed KDM3A and silenced EZH1 (Fig. 6A-6D).

In order to further determine that glioblastoma-EVs miR-27a-3p functioned as an upstream regulator of EZH1/KDM3A/CTGF in M2 macrophage polarization, CTGF was overexpressed in macrophages, followed by the detection of miR-27a-3p/EZH1/KDM3A/CTGF expression in each group. The results showed that the expression of miR-27a-3p, EZH1, KDM3A in the oe-CTGF group was basically unchanged compared with the oe-NC group. However, CTGF and IL-10 expression was increased and TNF-α expression was decreased after CTGF was overexpressed, along with induced M2 macrophage polarization (Fig. 6E-6G). EVs were extracted from miR-27a-3p mimic/miR-27a-3p inhibitor treated glioblastoma cells, which were co-cultured with CTGF overexpression vector (oe-CTGF)-treated macrophages. The results showed that the in EVs extracted from miR-27a-3p mimic-treated glioblastoma cells, upregulated CTGF prominently stimulated M2 macrophage polarization, in which the expression of miR-27a-3p, KDM3A and CTGF expression increased, but EZH1 and TNF-α expression reduced. In contrast, in the EVs extracted from miR-27a-3p inhibitor-treated cells, upregulated CTGF by oe-CTGF dampened M2 macrophage polarization, in which the miR-27a-3p, KDM3A, CTGF and IL-10 expression reduced, while EZH1 and TNF-α expression increased (Fig. 6H-6J). Besides, expression of iNOS and Arg-1 was measured using Western blotting, he results of which showed that the expression of iNOS decreased and Arg-1 increased in the glioblastoma-EVs containing miR-27a-3p mimic and macrophages

overexpressing CTGF. However, the results were reversed in the glioblastoma-EVs containing miR-27a-3p inhibitor and macrophages overexpressing CTGF (Fig. 6K).

The role of conditioned macrophages in the migration, invasion and proliferation of glioblastoma cells was further explored *in vitro*. The results of CCK-8 and Transwell assays showed that in glioblastoma-EVs containing miR-27a-3p mimic and macrophages overexpressing CTGF, strengthened proliferation, invasion and migration ability was observed, which was abolished in glioblastoma-EVs containing miR-27a-3p inhibitor and macrophages overexpressing CTGF (Fig. 6L-6N). These results suggest that glioblastoma-EVs carrying miR-27a-3p promote the activation of CTGF by inhibiting EZH1 expression and upregulating KDM3A, which in turn boost M2 macrophage polarization and ultimately facilitate the proliferation, migration and invasion of glioblastoma cells *in vitro*.

M2 macrophage polarization aggravates glioma progression in vivo

To validate the above-mentioned results *in vivo*, nude mice were injected with glioblastoma cells overexpressing miR-27a-3p or/and macrophages transfected with lentivirus-mediated CTGF to develop xenograft tumors. The results of RT-qPCR showed higher transfection efficiency of miR-27a-3p with CTGF (Fig. 7A). Results of HE staining exhibited that the boundary of mouse brain tissues was blurred after treatment of miR-27a-3p overexpression, accompanied with elevated invasive ability of glioblastoma cells. While the invasive ability of tumors to brain tissues was weaker in mice after CTGF expression was silenced (Fig. 7B). In addition, the survival time of mice was shortened after in glioblastoma cells overexpressing miR-27a-3p was injected into mice, while the survival time of mice was prolonged after interfering with CTGF (Fig. 7C). Results of Western blotting displayed that overexpression of miR-27a-3p led to downregulated EZH1 and upregulated KDM3A and CTGF. However, after silencing of CTGF, the expression of EZH1 and KDM3A did not change significantly, while the expression of CTGF was downregulated (Fig. 7D). The secretion levels of IL-10 and TNF-α in peripheral serum of mice were detected by ELISA. The results showed that the overexpression of miR-27a-3p resulted in the increase of IL-10 and the decrease of TNF-α, indicating that M2 polarization was induced in mice. However, the decrease of IL-10 and the increase of TNF-α were observed after silencing of CTGF, suggesting that loss of CTGF could prevent M2 macrophages polarization (Fig. 7E). These results suggest that glioblastoma-EVs promote the development of glioblastoma *in vivo* by reprogramming M2 macrophages.

Discussion

EVs activating macrophages is now considered as key players in cancer progression, as macrophages are able to promote the growth of tumors [15]. Moreover, hypoxia condition is likely to stimulate glioblastoma cells to secrete EVs, hence promoting the glioblastoma cell motility [16]. This study investigated the effects and mechanism of miR-27a-3p derived from glioblastoma-EVs on M2 macrophage polarization. We found that glioblastoma-EVs could deliver miR-27a-3p to participate in the polarization of M2 macrophage, thereby playing a key role in tumor microenvironment.

In the present study, we initially revealed that glioblastoma-EVs could deliver miR-27a-3p to polarize M2 macrophage. Coincidentally, EVs derived from monocytes containing miR-27a also play promoting role in the polarization of M2 macrophages [17]. Moreover, miR-27a that promotes proliferation and migration of glioblastoma cells is abundant in glioblastoma-EVs [18]. These works further support our statement that miR-27a-3p contained in glioblastoma-EVs could polarize M2 macrophage. Furthermore, miR-27a-3p expression was silenced by using plasmid of miR-27a-3p inhibitor. We found that loss of miR-27a-3p could upregulate the protein level of iNOS but downregulate Arg-1. It is reported that iNOS is one of the phenotypes of M1 macrophage while Arg-1 was a marker for M2 macrophage [19]. Therefore, it can be inferred that inhibited miR-27a-3p could curtail the M2 macrophage polarization.

We next found that miR-27a-3p could suppress the expression of EZH1, the target of miR-27a-3p. EZH1 is reported to participate in the macrophage phenotype shifting and downregulation of EZH1 is able to promote M2 macrophage [13]. To our best knowledge, the relationship between miR-27a-3p and EZH1 is barely explored in previous literature. Furthermore, we found that EZH1 could participate in the regulation of M2 polarization in association with KDM3A. Prior work also demonstrates that EZH1, as a H3K27me3 methylase, binds to the downstream gene promoter and promotes H3K27me3 to suppress gene expression [20], which is in line with our study proposing that EZH1 could inhibit the expression of KDM3A. As prior work verified, M2 macrophage can be induced by KDM3A [21]. Additionally, it is addressed that KDM3A, a demethylase of histone H3K9me1/2, can promote the expression of CTGF by facilitating H3K27ac on the enhancers of CTGF [22]. While CTGF promotes drug-resistance in glioblastoma cells and facilitates the progression of glioblastoma [23]. Based on what has been discussed above, it was indicated that miR-27a-3p secreted from glioblastoma-EVs could downregulate EZH1 expression, elevate expression of KDM3A and further upregulate CTGF to polarize M2 macrophage.

In vitro analysis further unraveled that proliferation, migration and invasion of glioblastoma cells were expedited by overexpressed miR-27a-3p and the underlying mechanism. Promoted M2 macrophage is associated with the enhanced proliferation and migration abilities of glioblastoma cells [24]. To confirm our results *in vivo*, we also employed murine glioblastoma cell line GL261 for generating xenograft rat models to study the effects of miR-27a-3p/EZH1/KDM3A/CTGF on development of glioblastoma *in vivo*. The data of our study displayed that overexpressed miR-27a-3p induced upregulated IL-10 and downregulated TNF-α in peripheral serum of mice. Promoted M2 macrophage polarization is related to increased expression of IL-10 and decreased expression of the pro-inflammatory cytokine TNF-α [25]. Therefore, the results derived from *in vitro* analysis were consistent with what we had concluded from *in vivo* experiment.

Conclusions

In summary, the evidence collected from our study collaboratively suggests that miR-27a-3p contained in glioblastoma-EVs inhibits the expression of target gene EZH1 to upregulate KDM3A-mediated CTGF expression, which induces M2 macrophage polarization and further facilitates proliferation, migration and invasion of glioblastoma cells (Figure 8). Our findings show that the glioblastoma-EVs miR-27a-3p

may be a biomarker for diagnosis of glioblastoma. It is likely that inhibition of miR-27a-3p in glioblastoma-EVs could serve as a tool to combat glioblastoma. Further studies of the molecular mechanisms underlying tumor-associated macrophage *via* the EVs will facilitate better understanding of the effects of glioblastoma-EVs on the progression of glioblastoma.

Declarations

Acknowledgments

We would also like to thank all participants enrolled in the present study.

Funding

This study was supported by the National Natural Science Foundation of China (81901972, 81201671), and Foundation of Science and Technology Department of Jilin Province (20180101306JC, 20190201090JC).

Availability of data and materials

The authors confirm that the data supporting the findings of this study are available within the article.

Ethics approval and consent to participate

The usage of cerebrospinal fluid and tumor tissues was approved by the Institutional review board (IRB) of the Jilin University. The study protocol was authorized by the IRB of the Jilin University. with patient's written informed consent obtained. This study was performed in compliance with the *Declaration of Helsinki*. The animal experiments were approved by the Animal Ethics Committee of the Jilin University.

Consent for publication

Not applicable.

Authors' contributions

Guifang Zhao and Hongquan Yu wrote the paper; Lijuan Ding and Weiyao Wang conceived the experiments; Huang Wang, Yao Hu and Lingsha Qin analyzed the data; Guangce Deng, Buqing Xie, Guofeng Li and Ling Qi collected and provided the sample for this study. All authors have read and approved the final submitted manuscript.

Competing interests

The authors declare that they have no competing interests.

Abbreviations

miRNA (microRNA); glioblastoma-EVs (extracellular vesicles of glioblastoma); TEM (transmission electron microscopy); NTA (Nano-particle tracking analysis); EZH1 (enhancer of zeste homologue 1);

CTGF (connective tissue growth factor); HE (hematoxylin-eosin); IRB (Institutional review board); FBS (fetal bovine serum); RPMI (Roswell Park Memorial Institute); PMA (phorbol-myristate-acetate); STR (short tandem repeat); siRNA (Small interfering RNA); TEM (Transmission electron microscope).

References

1. Ostrom QT, Gittleman H, Xu J, Kromer C, Wolinsky Y, Kruchko C *et al*: CBTRUS Statistical Report: Primary Brain and Other Central Nervous System Tumors Diagnosed in the United States in 2009-2013. Neuro Oncol. 2016;18:v1-v75.
2. Gularyan SK, Gulin AA, Anufrieva KS, Shender V, Shakhparonov MI, Bastola S *et al*: Investigation of inter- and intra-tumoral heterogeneity of glioblastoma using TOF-SIMS. Mol Cell Proteomics. 2020;
3. Wang Y, Zhao B, Chen W, Liu L, Chen W, Zhou L *et al*: Pretreatment Geriatric Assessments of Elderly Patients with Glioma: Development and Implications. Aging Dis. 2020;11:448-61.
4. Lu J, Xu Z, Duan H, Ji H, Zhen Z, Li B *et al*: Tumor-Associated Macrophage IL-1beta Promotes GPD2 Activation, Glycolysis, and Tumorigenesis in Glioma Cells. Cancer Sci. 2020;
5. Hernandez-SanMiguel E, Gargini R, Cejalvo T, Segura-Collar B, Nunez-Hervada P, Hortiguela R *et al*: Ocoxin Modulates Cancer Stem Cells and M2 Macrophage Polarization in Glioblastoma. Oxid Med Cell Longev. 2019;2019:9719730.
6. Yekula A, Yekula A, Muralidharan K, Kang K, Carter BS, Balaj L: Extracellular Vesicles in Glioblastoma Tumor Microenvironment. Front Immunol. 2019;10:3137.
7. Qian M, Wang S, Guo X, Wang J, Zhang Z, Qiu W *et al*: Hypoxic glioma-derived exosomes deliver microRNA-1246 to induce M2 macrophage polarization by targeting TERF2IP via the STAT3 and NF-kappaB pathways. Oncogene. 2020;39:428-42.
8. Hayes J, Peruzzi PP, Lawler S: MicroRNAs in cancer: biomarkers, functions and therapy. Trends Mol Med. 2014;20:460-9.
9. Mittelbrunn M, Gutierrez-Vazquez C, Villarroya-Beltri C, Gonzalez S, Sanchez-Cabo F, Gonzalez MA *et al*: Unidirectional transfer of microRNA-loaded exosomes from T cells to antigen-presenting cells. Nat Commun. 2011;2:282.
10. An T, Fan T, Zhang XQ, Liu YF, Huang J, Liang C *et al*: Comparison of Alterations in miRNA Expression in Matched Tissue and Blood Samples during Spinal Cord Glioma Progression. Sci Rep. 2019;9:9169.
11. Perge P, Decmann A, Pezzani R, Bancos I, Fassina A, Luconi M *et al*: Analysis of circulating extracellular vesicle-associated microRNAs in cortisol-producing adrenocortical tumors. Endocrine. 2018;59:280-87.
12. Li G, Warden C, Zou Z, Neman J, Krueger JS, Jain A *et al*: Altered expression of polycomb group genes in glioblastoma multiforme. PLoS One. 2013;8:e80970.
13. Jia X, Xu H, Miron RJ, Yin C, Zhang X, Wu M *et al*: EZH1 Is Associated with TCP-Induced Bone Regeneration through Macrophage Polarization. Stem Cells Int. 2018;2018:6310560.

14. Wang Z, Li S, Wang Y, Zhang X, Chen L, Sun D: GDNF enhances the anti-inflammatory effect of human adipose-derived mesenchymal stem cell-based therapy in renal interstitial fibrosis. Stem Cell Res. 2019;41:101605.
15. Chanmee T, Ontong P, Konno K, Itano N: Tumor-associated macrophages as major players in the tumor microenvironment. Cancers (Basel). 2014;6:1670-90.
16. Kucharzewska P, Christianson HC, Welch JE, Svensson KJ, Fredlund E, Ringner M *et al*: Exosomes reflect the hypoxic status of glioma cells and mediate hypoxia-dependent activation of vascular cells during tumor development. Proc Natl Acad Sci U S A. 2013;110:7312-7.
17. Saha B, Momen-Heravi F, Kodys K, Szabo G: MicroRNA Cargo of Extracellular Vesicles from Alcohol-exposed Monocytes Signals Naive Monocytes to Differentiate into M2 Macrophages. J Biol Chem. 2016;291:149-59.
18. Monteforte A, Lam B, Sherman MB, Henderson K, Sligar AD, Spencer A *et al*: (*) Glioblastoma Exosomes for Therapeutic Angiogenesis in Peripheral Ischemia. Tissue Eng Part A. 2017;23:1251-61.
19. Jin Z, Li J, Pi J, Chu Q, Wei W, Du Z *et al*: Geniposide alleviates atherosclerosis by regulating macrophage polarization via the FOS/MAPK signaling pathway. Biomed Pharmacother. 2020;125:110015.
20. Shen X, Liu Y, Hsu YJ, Fujiwara Y, Kim J, Mao X *et al*: EZH1 mediates methylation on histone H3 lysine 27 and complements EZH2 in maintaining stem cell identity and executing pluripotency. Mol Cell. 2008;32:491-502.
21. Liu X, Chen J, Zhang B, Liu G, Zhao H, Hu Q: KDM3A inhibition modulates macrophage polarization to aggravate post-MI injuries and accelerates adverse ventricular remodeling via an IRF4 signaling pathway. Cell Signal. 2019;64:109415.
22. Wang HY, Long QY, Tang SB, Xiao Q, Gao C, Zhao QY *et al*: Histone demethylase KDM3A is required for enhancer activation of hippo target genes in colorectal cancer. Nucleic Acids Res. 2019;47:2349-64.
23. Zeng H, Yang Z, Xu N, Liu B, Fu Z, Lian C *et al*: Connective tissue growth factor promotes temozolomide resistance in glioblastoma through TGF-beta1-dependent activation of Smad/ERK signaling. Cell Death Dis. 2017;8:e2885.
24. Bao L, Li X: MicroRNA-32 targeting PTEN enhances M2 macrophage polarization in the glioma microenvironment and further promotes the progression of glioma. Mol Cell Biochem. 2019;460:67-79.
25. Bi C, Fu Y, Li B: Brain-derived neurotrophic factor alleviates diabetes mellitus-accelerated atherosclerosis by promoting M2 polarization of macrophages through repressing the STAT3 pathway. Cell Signal. 2020;70:109569.

Figures

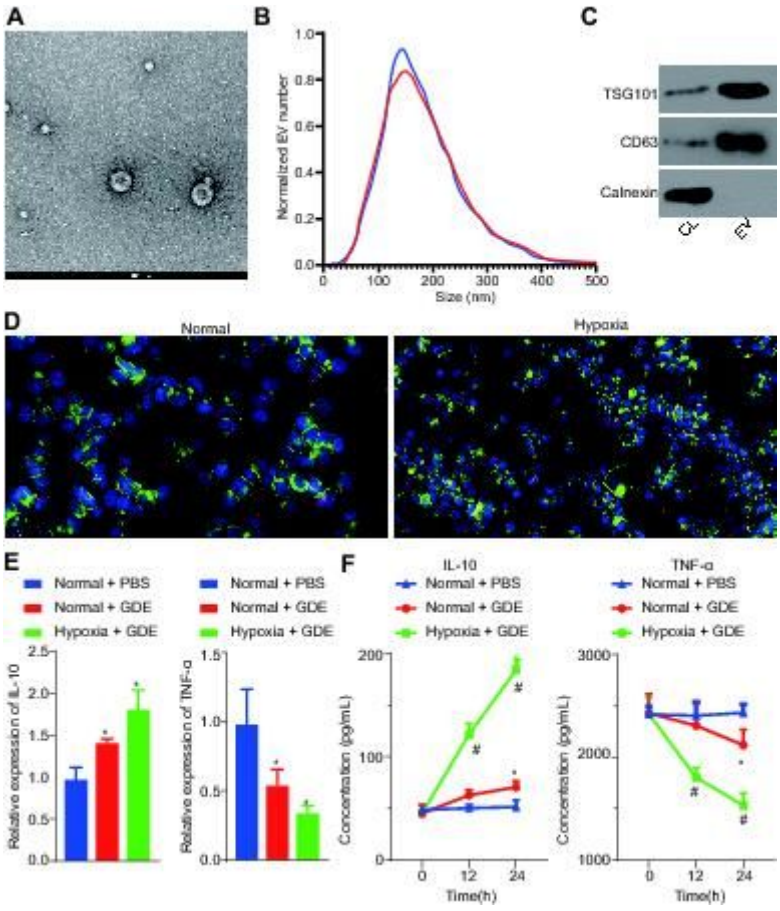

Figure 1

Glioblastoma-EVs promote M2 polarization. A, TEM results of glioblastoma-EVs (200 nm). B, NAT results of the size distribution of EVs. C, Expression of marker proteins TSG101, CD63 and Calnexin in glioblastoma-EVs and cell lysates determined using Western blotting. D, Immunofluorescence images of EV uptake by macrophages under normoxia/hypoxia (double label; Color red represents EVs; Color green indicates macrophage; 600 x). E, RT-qPCR results of IL-10 and TNF-α expression in macrophages. F, ELISA results of the secretion levels of IL-10 and TNF-α in the supernatant of macrophages. * $p < 0.05$ compared with the normal cells treated with PBS. # $p < 0.05$ compared with normal cells treated with glioblastoma-EVs. Measurement data are expressed by mean ± standard deviation. One-way ANOVA is used for comparison among multiple groups and Tukey's post hoc test. Comparison among groups at different time points is conducted using two-way ANOVA and Bonferroni's post hoc test.

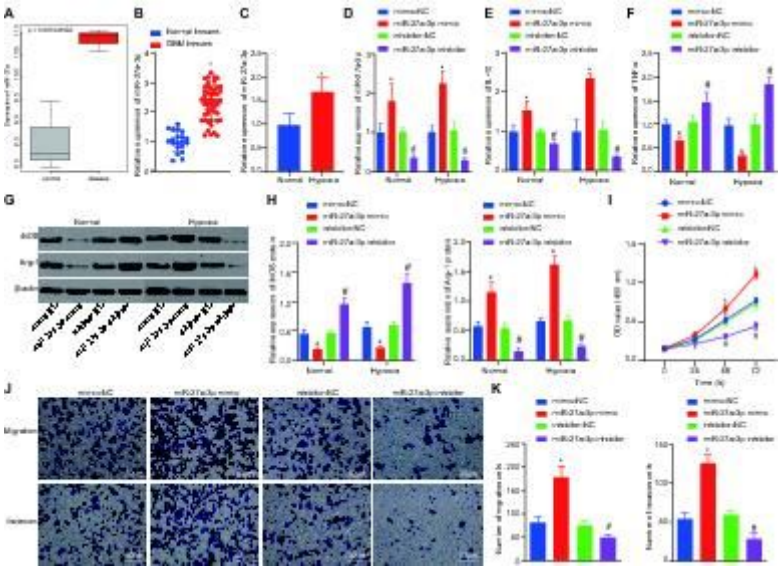

Figure 2

Glioblastoma-EVs transfer miR-27a-3p to macrophages to induce M2 polarization. A, Differential expression of miR-27a-3p in microarray GSE65626. The X-axis represents sample type, and the Y-axis represents expression value. Gray box indicates normal sample, while red box indicates tumor sample. B, RT-qPCR results of miR-27a-3p expression in clinical samples of glioblastoma patients (n = 50) and non-glioblastoma patients (n = 20). C, RT-qPCR results of miR-27a-3p expression in macrophages cultured under normoxia/hypoxia conditions. D, E and F, Expression of miR-27a-3p, IL-10 and TNF-α in macrophages treated with miR-27a-3p mimic/miR-27a-3p inhibitor under normoxia/hypoxia conditions. G and H, Western blotting results of the protein expression of iNOS and Arg-1. I, The proliferative ability of glioblastoma cells detected by CCK-8 assay. J and K, Transwell assay results of migration and invasion ability of glioblastoma cells. * $p < 0.05$ compared with normal tissues, normal cells or macrophages treated with mimic-NC. # $p < 0.05$ compared with macrophages treated with inhibitor-NC. Measurement data are expressed by mean ± standard deviation. Data in two different groups are compared using unpaired t-test. One-way ANOVA is used for comparison among multiple groups and Tukey's post hoc test. Comparison among groups at different time points is conducted using two-way ANOVA and Bonferroni's post hoc test.

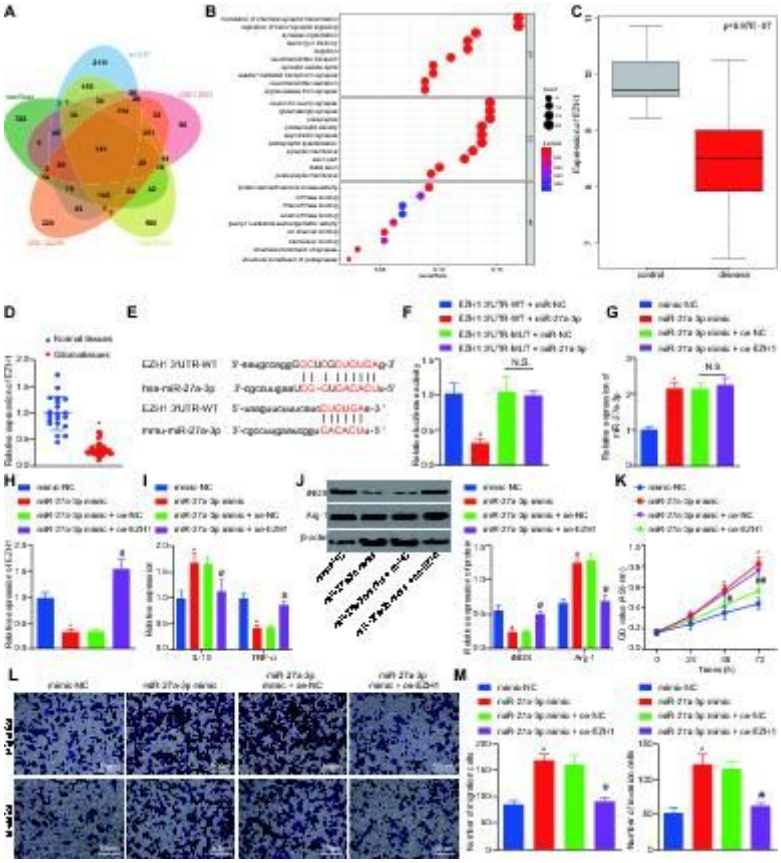

Figure 3

miR-27a-3p targets EZH1 to induce M2 polarization. A, Target genes of miR-27a-3p predicted by bioinformatics analysis. The five ellipses represent the database prediction results and the differentially expressed genes in the glioblastoma-related microarrays. The intersected results are shown in the middle part. B, GO functional enrichment analysis on the intersected genes. X-axis represents gene ratio.Y-axis represents GO entries. The right histogram is color gradation. C, The expression of EZH1 in microarray GSE50161. D, The expression of EZH1 in clinical samples of glioblastoma patients (n = 50) and non-glioblastoma patients (n = 20). E, The binding sites between miR-27a-3p and EZH1 3'UTR in human and mice predicted by starBase databse. F, The targeting relationship between miR-27a and EZH1 verified by dual luciferase reporter gene assay. G, H and I, The expression of miR-27a-3p, EZH1, IL-10, TNF-α in macrophages cultured under hypoxic conditions. J, The protein expression of iNOS and Arg-1 determined by Western blotting. K, The proliferation ability of glioblastoma cells evaluated by CCK-8 assay. L and M, The migration and invasion ability of glioblastoma cells assessed by Transwell assay. * $p < 0.05$ compared with the mimic-NC group. # $p < 0.05$ compared with miR-27a-3p mimic + oe-NC group. Measurement data are expressed by mean ± standard deviation. Data in two different groups are compared using unpaired t-test. One-way ANOVA is used for comparison among multiple groups and Tukey's post hoc test. Comparison among groups at different time points is conducted using two-way ANOVA and Bonferroni’s post hoc test.

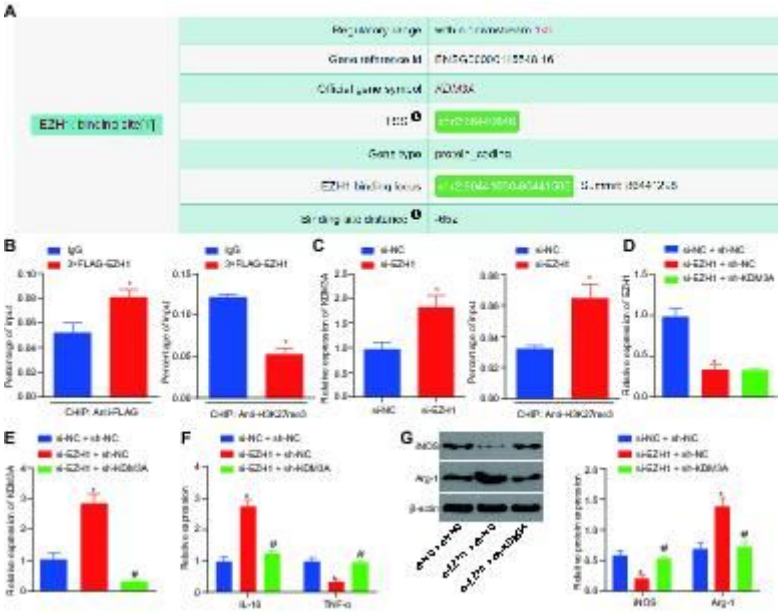

Figure 4

miR-27a-3p targets EZH1 to induce M2 polarization. A, Target genes of miR-27a-3p predicted by bioinformatics analysis. The five ellipses represent the database prediction results and the differentially expressed genes in the glioblastoma-related microarrays. The intersected results are shown in the middle part. B, GO functional enrichment analysis on the intersected genes. X-axis represents gene ratio.Y-axis represents GO entries. The right histogram is color gradation. C, The expression of EZH1 in microarray GSE50161. D, The expression of EZH1 in clinical samples of glioblastoma patients (n = 50) and non-glioblastoma patients (n = 20). E, The binding sites between miR-27a-3p and EZH1 3'UTR in human and mice predicted by starBase databse. F, The targeting relationship between miR-27a and EZH1 verified by dual luciferase reporter gene assay. G, H and I, The expression of miR-27a-3p, EZH1, IL-10, TNF-α in macrophages cultured under hypoxic conditions. J, The protein expression of iNOS and Arg-1 determined by Western blotting. K, The proliferation ability of glioblastoma cells evaluated by CCK-8 assay. L and M, The migration and invasion ability of glioblastoma cells assessed by Transwell assay. * $p < 0.05$ compared with the mimic-NC group. # $p < 0.05$ compared with miR-27a-3p mimic + oe-NC group. Measurement data are expressed by mean ± standard deviation. Data in two different groups are compared using unpaired t-test. One-way ANOVA is used for comparison among multiple groups and Tukey's post hoc test. Comparison among groups at different time points is conducted using two-way ANOVA and Bonferroni’s post hoc test.

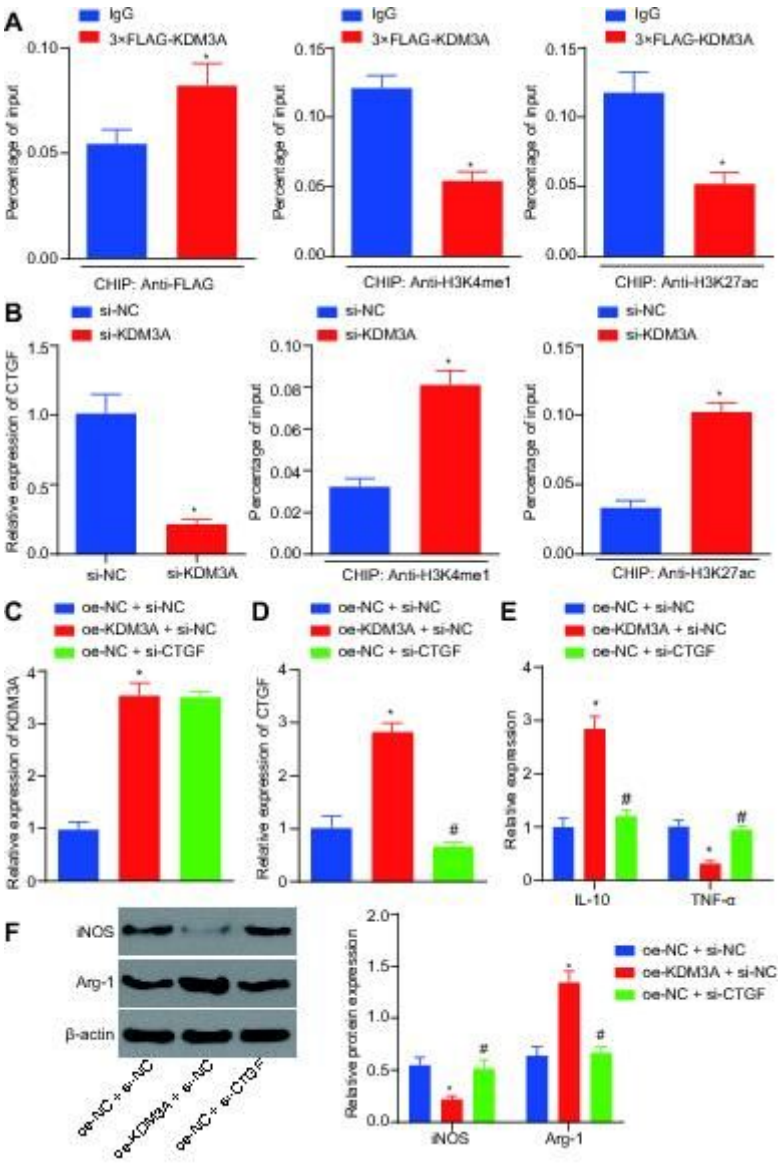

Figure 5

miR-27a-3p targets EZH1 to induce M2 polarization. A, Target genes of miR-27a-3p predicted by bioinformatics analysis. The five ellipses represent the database prediction results and the differentially expressed genes in the glioblastoma-related microarrays. The intersected results are shown in the middle part. B, GO functional enrichment analysis on the intersected genes. X-axis represents gene ratio.Y-axis represents GO entries. The right histogram is color gradation. C, The expression of EZH1 in microarray GSE50161. D, The expression of EZH1 in clinical samples of glioblastoma patients (n = 50) and non-glioblastoma patients (n = 20). E, The binding sites between miR-27a-3p and EZH1 3'UTR in human and mice predicted by starBase databse. F, The targeting relationship between miR-27a and EZH1 verified by dual luciferase reporter gene assay. G, H and I, The expression of miR-27a-3p, EZH1, IL-10, TNF-α in macrophages cultured under hypoxic conditions. J, The protein expression of iNOS and Arg-1 determined by Western blotting. K, The proliferation ability of glioblastoma cells evaluated by CCK-8 assay. L and M, The migration and invasion ability of glioblastoma cells assessed by Transwell assay. * $p < 0.05$ compared with the mimic-NC group. # $p < 0.05$ compared with miR-27a-3p mimic + oe-NC group.

Measurement data are expressed by mean ± standard deviation. Data in two different groups are compared using unpaired t-test. One-way ANOVA is used for comparison among multiple groups and Tukey's post hoc test. Comparison among groups at different time points is conducted using two-way ANOVA and Bonferroni's post hoc test.

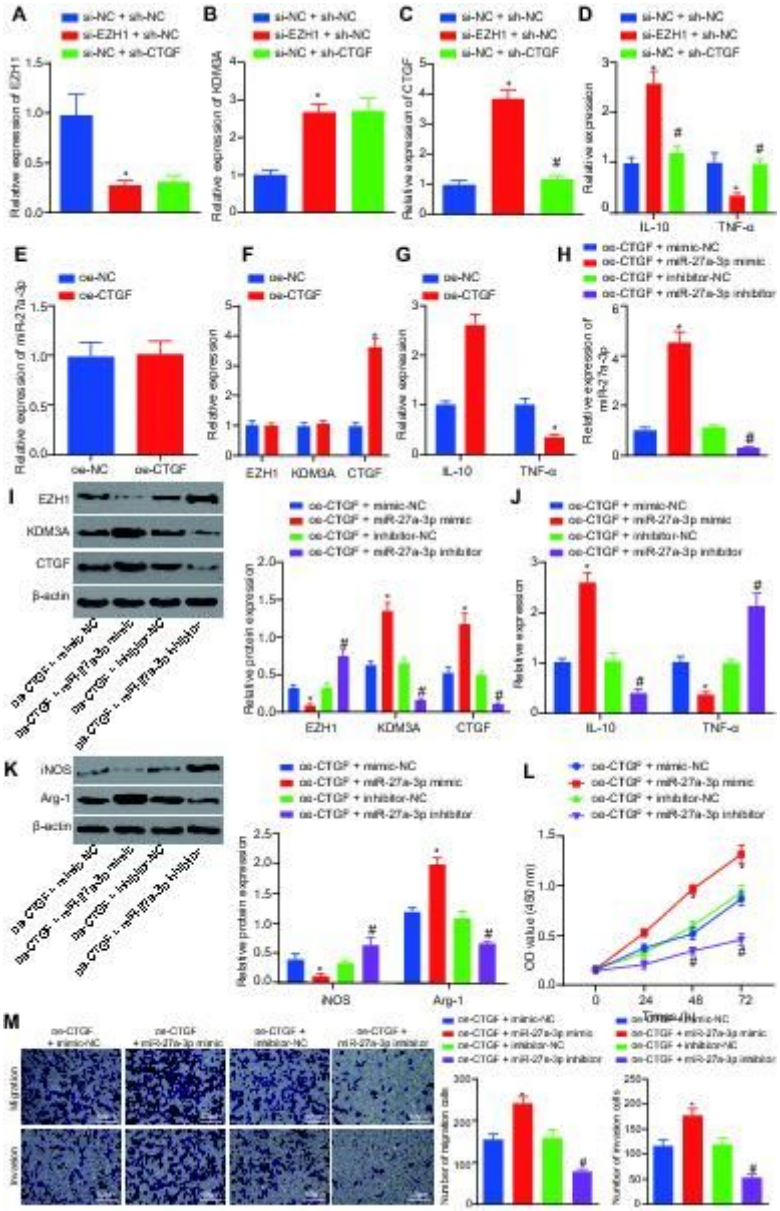

Figure 6

miR-27a-3p contained in glioblastoma-EVs targets EZH1 to mediate M2 polarization through KDM3A/CTGF in vitro. A-D, Expression of EZH1, KDM3A and CTGF in macrophages after EZH1 and CTGF knockdown determined using RT-qPCR. E, F and G, Expression of EZH1, KDM3A and CTGF in macrophages overexpressing CTGF evaluated using RT-qPCR. H, Expression of miR-27a-3p after macrophages were transfected with miR-27a-3p mimic/inhibitor determined using RT-qPCR. I, Protein expression of EZH1, KDM3A and CTGF measured using Western blotting. J, Expression of IL-10 and TNF-α detected using RT-qPCR. K, Protein expression of iNOS and Arg-1 determined using Western blotting. L, CCK-8 assay results of proliferation ability of glioblastoma cells. M and N, Transwell assay results of the

migration and invasion ability of glioblastoma cells.* p < 0.05 compared with si-NC + sh-NC, oe-NC or oe-CTGF + mimic-NC. # p < 0.05 compared with oe-CTGF + inhibitor-NC. Measurement data are expressed by mean ± standard deviation. Data in two different groups are compared using unpaired t-test. One-way ANOVA is used for comparison among multiple groups and Tukey's post hoc test. Comparison among groups at different time points is conducted using two-way ANOVA and Bonferroni's post hoc test.

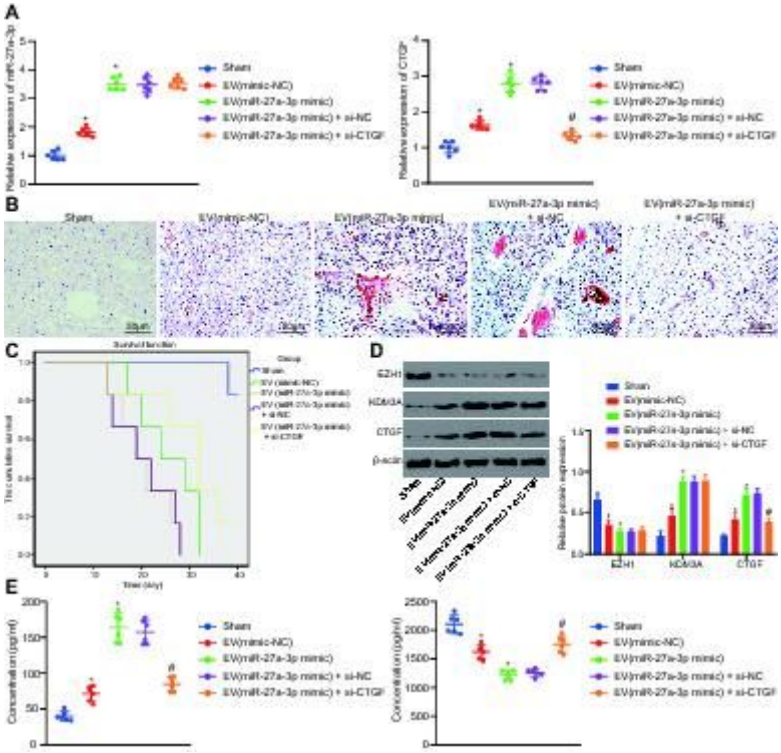

Figure 7

Glioblastoma can be aggravated by miR-27a-3p contained in glioblastoma-EVs in vivo. A, Expression of miR-27a-3p and CTGF in each group of mice (n = 60) determined using RT-qPCR after the mouse model was treated with glioblastoma cells overexpressing miR-27a-3p or silencing CTGF. B, HE staining results of glioblastoma cell invasion to the mouse brain tissues (n = 60). C, Statistical data of survival time of mice in each group (n = 60). D, Western blotting results of the protein expression of EZH1, KDM3A and CTGF in mice of each group. E, ELISA results of secretion levels of IL-10 and TNF-α in peripheral serum of mice. * p < 0.05 compared with sham-operated mice. # p < 0.05 compared with EVs containing miR-27a-3p mimic + si-NC group.

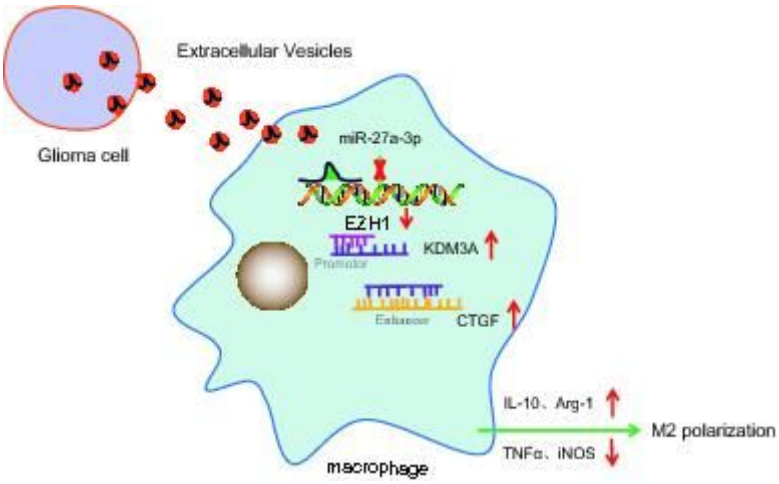

Figure 8

Schematized molecular mechanism underlying miR-27a-3p contained in glioblastoma-EVs. EV miR-27a-3p inhibits the expression of target gene EZH1 to upregulate KDM3A-mediated CTGF expression, which induces M2 macrophage polarization and further facilitates proliferation, migration and invasion of glioblastoma cells.